Int. J. Heat Mass Transfer. Vol. 36, No. 2, pp. 325–335, 1993
Printed in Great Britain

0017-9310/93 $6.00 + 0.00

Critical heat flux for low flow boiling in vertical uniformly heated thin rectangular channels

CHANG H. OH† and STAN B. ENGLERT
Idaho National Engineering Laboratory, EG&G Idaho, Inc., Thermal Analysis Unit, PO Box 1625, Idaho Falls, ID 83415, U.S.A.

(*Received* 8 *November* 1991 *and in final form* 6 *March* 1992)

Abstract—Steady-state, subcooled, low flow, critical heat flux (CHF) experiments simulating natural convection boiling are performed in a thin rectangular vertical channel. The aluminum channel is heated on one side; the other side of the channel is a Pyrex window allowing visual observation of the CHF event. Both upward and downward flow conditions are tested with exit pressure varying from 20 to 85 kPa, inlet water temperature varying from 295 to 343 K (inlet subcooling = 5–72 K), and mass flux varying from 30 to 80 kg s^{-1} m^{-2}. Measured test results indicate downward flow dryout CHF occurring at 85% of upward flow dryout CHF values. This percentage is believed to result from the flow instability and reduced inlet subcooling induced by the counter-current flow. New dryout CHF correlations for low flow rates, representative of natural convection boiling, are recommended for both upward and downward flow.

INTRODUCTION

THE OCCURRENCE of burnout during natural convection boiling can be very important to the safety of plate-type reactors, like the advanced test reactor (ATR) and the material test reactor (MTR) under accident conditions such as loss-of-coolant accidents (LOCAs) and complete loss-of-flow accidents (CLOFAs). Under such accident conditions, insufficient decay heat removal via the thin flow channel can be detrimental to the normal boiling heat transfer process, resulting in burnout at the low heat fluxes. A CLOFA analysis [1] for the ATR indicated that natural convection boiling was quickly established (within 20 s) in the reactor vessel once the forced flow was stopped. Therefore, when the flow reverses during the transient, burnout or critical heat flux (CHF) may occur if the flow rate is insufficient to remove the decay heat. Most CHF studies reported in the cited literature [2–9] are based on high pressure boiling heat transfer in round tubes or rod bundles. Critical heat flux data on the rectangular channel under low flow and low pressure are scarce, and most recent studies [10–17] are limited to atmospheric pressure and a stainless steel, heated surface. A LOCA study for the ATR indicated that the system pressure dropped to 20 kPa 5 s after a large pipe break [18]. The CHF study needs to be extended for the low pressure range where natural convection boiling becomes more important. Furthermore, because the CHF depends on localized boiling conditions that are influenced by the surface condition, geometry, and ranges of the operating variables, understanding the role of these pertinent parameters is essential to understanding the CHF phenomena.

† Author to whom correspondence should be addressed.

Different heated surface materials were studied by Tachibana *et al.* [19], Van Ouwerkerk [20] and Knoebel *et al.* [3]. In pool boiling tests, Tachibana *et al.* measured CHF for different materials: stainless steel, nickel, and copper. Tachibana *et al.* found that aluminum had a 25% higher CHF than stainless steel at equivalent conditions.

In a pool boiling stability study, Van Ouwerkerk found that the high heat-conducting surface of aluminum had characteristically higher CHF. Knoebel *et al.* also found that aluminum CHF data were 22% higher than stainless steel data for equivalent conditions. CHF correlations specifically for an aluminum surface, however, were not found in current published literature for low pressure and low flow conditions.

The purpose of this study was to measure low flow (typical of natural convection in the ATR) and low pressure CHF, and to recommend a CHF correlation.

A comparison study between the forced convection boiling CHF and the natural convection boiling CHF at flow rates up to 76 kg s^{-1} m^{-2} was performed by Mishima and Ishii [12]. The study indicated that natural convection boiling CHF values were about the same as forced convection boiling CHF values. Based on Mishima and Ishii's study, the mass velocity in this present study was maintained low enough to mimic natural convection boiling. Forced flow was used to control the flow rate as precisely as possible.

BACKGROUND

CHF has been extensively studied for the past three decades. Among almost 400 CHF correlations in published literature, only a few correlations are appropriate for low flow rates in thin rectangular channels.

Mishima and Nishihara [10] carried out CHF tests

NOMENCLATURE

A	flow area [m^2]
A_h	heat transfer area [m^2]
A_1	constant in equation (3)
B_1	constant in equation (3)
C_0	void distribution parameter
C_1	constant in equation (3)
D	diameter [m]
D_e	equivalent diameter based on wetted perimeters [m]
D^*	dimensionless diameter
D_1	constant in equation (4)
E_1	constant in equation (4)
G	mass flux [kg s^{-1} m^{-2}]
G^*	dimensionless mass flux
g	acceleration gravity [m s^{-2}]
h_{fg}	latent heat of evaporation [kJ kg^{-1}]
Δh_i	inlet subcooling [kJ kg^{-1}]
L	length [m]
q^*	dimensionless heat flux
Q	total heat input [kW]
ΔT_{sub}	inlet subcooling [K].

Greek symbols

Δ	difference between liquid and gas
λ	Taylor wavelength [m]
ρ	density [kg m^{-3}]
σ	surface tension [N m^{-1}].

Subscripts

f	liquid
g	gas, steam.

using a thin rectangular vertical flow channel, 0.0024 m across the flow channel gap, 0.03 m wide, and 0.35 m long. Two stainless steel test sections were used in the study; one section was heated from one wide side while the other was heated from both wide sides. The mass flux varied from 0 to 360 kg s^{-1} m^{-2}; the inlet water temperature varied from 285 to 373 K; and the exit pressure was atmospheric for both upward and downward flow. The results indicated that CHF in the test section heated from both sides was about half that of the test section heated from one side. Mishima and Nishihara found that CHF for the test section heated from one side for downward flow with a mass flow rate of 100 kg s^{-1} m^{-2}, and an inlet water temperature between 301 and 306 K, was lower than that for upward flow by a factor of two.

Monde and Yamaji [11] carried out experiments similar to Mishima and Nishihara. Vertical tubes ($D = 0.00112$–0.0184 m) were submerged in three different liquids at atmospheric pressure. A parametric study of the ratio of the heated length over the diameter was performed and a generalized correlation was derived for natural convection boiling CHF. Two CHF correlations were developed depending on the characteristic criterion of $D/\sqrt{(\sigma/g(\rho_f-\rho_g))}$.

Mishima and Ishii [12] performed CHF experiments at low flow conditions for low pressure steam–water upward flow in an annulus that was formed by a 0.59 m long, 0.0204 m o.d. (outside diameter of the inside tube), directly heated, type 304 stainless steel tube, and a 0.9 m long, 0.0259 m i.d. (inside diameter of the outside tube) transparent Pyrex pipe. The mass flux of the natural convection boiling and the forced convection boiling varied from 0 to 35.8 kg s^{-1} m^{-2} at atmospheric pressure. Mishima and Ishii found that burnout at low flow rates occurred because of liquid film dryout during flow regime transition from the churn–turbulent to annular flow.

El-Genk *et al.* [13] carried out CHF experiments similar to those of Mishima and Ishii. The test section was made of 304 stainless steel with annulus ratios (o.d./i.d.) of 1.575 to 2. CHF correlations were developed according to flow transitions which occurred at CHF. They also studied CHF values for zero inlet flow using Block and Wallis' flooding correlations [21].

Katto [14] has extensively studied CHF for forced convection boiling in vertical, uniformly heated, round tubes from which he developed CHF correlations based on dimensional analysis. Katto collected CHF data using seven different fluids. His data were categorized into four flow regimes, and the corresponding correlations were developed according to the flow regime.

Kaminaga *et al.* [15] carried out CHF experiments for both upward and downward flow, with a non-uniform heat flux simulating a subchannel in a fuel element of Japan Research Reactor, JRR-3. The test section was made of Inconel 600 with a length of 0.00225 m flow gap, a 0.04 m heated width, and a 0.75 m heated length. The mass flux varied up to 300 kg s^{-1} m^{-2} with an inlet subcooling of 4–78 K. Lower CHF values were also observed for downward flow than for upward flow under equivalent conditions.

Macbeth [16] and Lowdermilk *et al.* [17] carried out CHF experiments using round tubes for a wide range of pressure and flow rates. Critical heat flux correlations developed for low flow and low pressure were chosen to estimate CHF in this present study.

EXPERIMENTAL APPARATUS AND PROCEDURE

The apparatus consists of the test section, a large cylindrical glass reservoir, a vacuum pump, associated piping, pressure transducers, values, and a centrifugal

pump to deliver a precisely controlled fluid flow to the test section. The test section is a thin rectangular aluminum channel heated on one side with Watlow firebar electrical strip heaters (11 kW capacity). The channel has a full-length Pyrex window, making the full test channel visible (a 0.00198 m flow gap, a 0.0508 m heated width, and a 0.6096 m heated length). Critical heat flux occurred at the exit of the flow direction where the exit pressure affects the dryout phenomena significantly. In order to maintain the same pressure drop for both upward and downward flow orientations, both upper and lower plenums were eliminated from our test loop. The apparatus can deliver forced vertical upward or downward flow to the test section, or permit natural circulation in the test section. Figure 1 is a schematic diagram of the test loop. Figure 2 is a cross section of the test section.

The ion-exchanged water flow in the test loop was established while evacuating the liquid reservoir. After observation of the reservoir liquid and test section pressure, which indicated clearly that the system was degassed, the test pressure was established, the Harrison model 6475 d.c. power supply (110 V d.c. and 100 A) was turned on and current was applied to the heater. Power to the test section was gradually increased by small steps until CHF occurred. The power was then turned down, estabiishing a new test condition.

Twenty-two chromel–alumel (C–A) type-K substrate thermocouples (TCs) were located as shown in Fig. 3. Both upward and downward flow conditions were tested with exit pressure varying from 20 to 85 kPa, inlet water temperature varying from 295 to 343 K (inlet subcooling = 5–72 K), and mass flux varying from 30 to 80 kg s^{-1} m^{-2}.

The data acquisition system was comprised of a Hewlett–Packard (H–P) 3497A data logger, Tektronix 4052 graphic computer, and a Tektronix 4907 disc drive and 4611 hard copy unit. The whole test data set (22 substrate TCs, the inlet/outlet water temperatures, the top/bottom reservoir pressure, and the ΔP across the test section) were recorded with a video recorder using a Sony model CCD-V101 color camera. The flow rate, pressure, and four test hot substrate temperatures (four TCs at the bottom for downward flow, or four TCs at the top for upward flow) also were recorded using a Soltec 6 channel analog strip chart recorder. The strip chart recorder provided supplementary evidence for determining a CHF condition.

When calibrated, the thermocouple measurements on both sides were in excellent agreement (within $\pm 0.2\%$) with tabulated values in the *OMEGA Temperature Handbook* over a temperature range of 283–800 K. The uncertainty in power reading was within a $\pm 0.10\%$ reading, turbine flowmeter (FMT-L5-M48) within $\pm 1.0\%$ reading, reservoir pressure within $\pm 0.5\%$, and Validyne differential pressure within $\pm 0.5\%$. Each test was repeated at the same condition to ensure repeatability of the tests within $\pm 2\%$.

DETERMINATION OF CHF CONDITION

At each test condition, power was applied in small increments, and the system was allowed to stabilize. As heater power increased, nucleate boiling occurred and flow regimes changed to bubble flow, then to churn flow, then to annular flow, and finally to annular flow with entrainment. During the transition from churn to annular flow, a great deal of bubble formation and collapse occurred. Critical heat flux was indicated by the combination of the following three

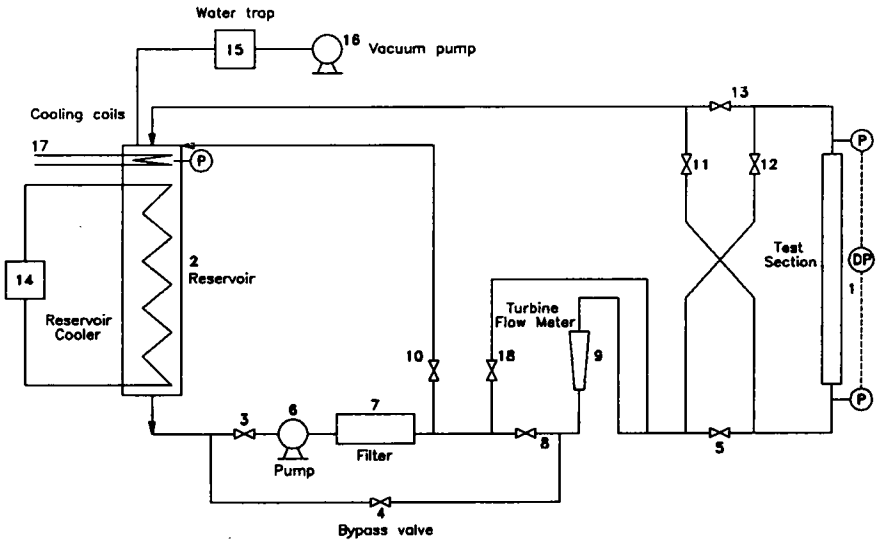

FIG. 1. Schematic diagram of test loop.

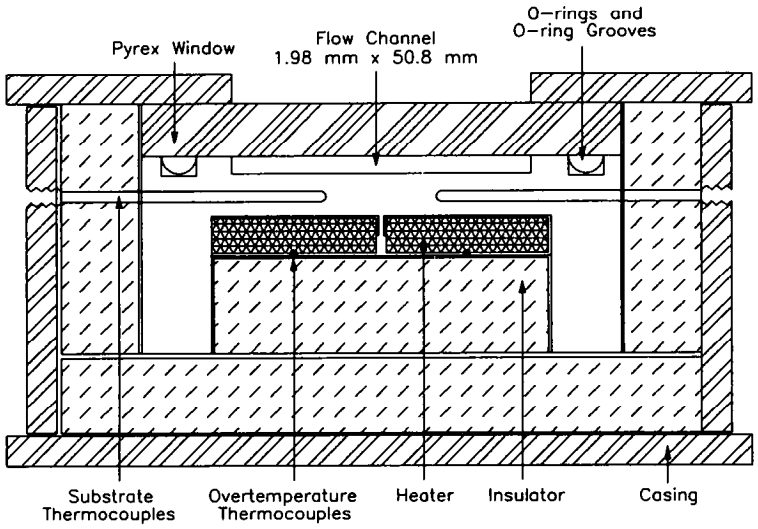

FIG. 2. Cross section of test section.

observations. First, the change in flow regimes led to subsequent dryout of the surface occurring over several minutes. (This dryout portion of the surface requenches several times in the very early stages. As power increases, the dryout does not requench and the dryout area increase.) Second, the hot spot substrate temperatures recorded on the strip chart drastically deviated from the pre-CHF oscillating temperatures and rapidly increased. (The amplitude in temperature oscillations varied from 3 to 15 K as CHF was approached. Critical heat flux was indicated by a sharp and continued departure from the indicated slope of the substrate temperature curves.) Third, the substrate temperatures recorded on digital data acquisition system rapidly increased. (At the onset of CHF, TCs at the dryout locations indicated a sharp and continued temperature increase.) During these tests, data were recorded on the strip chart from the data acquisition system by taking a single data scan. For selected tests, a video camera was also used to record CHF phenomena.

When the three observations were apparent, the condition was defined as CHF; CHF was calculated using the corresponding d.c. power supply voltage and current. Figure 4 shows a typical strip chart recording of the approach, onset, and development of CHF and power shutdown. Thermocouples L1, L2, L4, and L6 (see Fig. 3) are located at 0.0254, 0.0508, 0.102, and 0.152 m from the bottom left side of the heated test section. Again, as shown in Fig. 4, TC L1 showed an abrupt increase at CHF along with a significant increase in pressure drop across the test section.

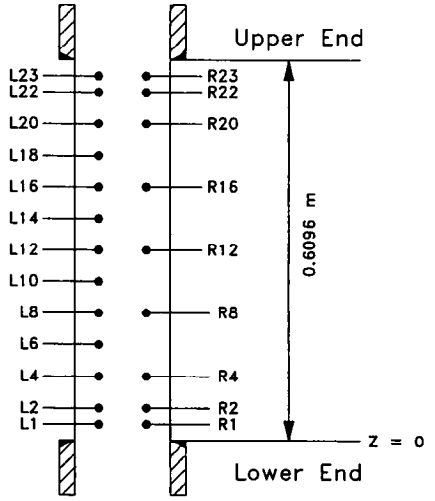

FIG. 3. Location of C–A thermocouples (the numbers denote the distance from $z = 0$ measured in inches).

EXPERIMENTAL RESULTS

A total number of 116 CHF data were collected. The experimental data consisted of two sets, one set for downward flow and the other for upward flow. For each data set, the inlet subcooling, system pressure, and the mass flow were varied. The data are shown as functions of the following important variables that affect the value of CHF: subcooling, pressure and mass flux.

Subcooling

Generally, the relationship between subcooling and CHF is linear. However, nonlinearity is possible depending on the flow regime and flow rate. Katto [14] analyzed the data collected from Macbeth [16] and Lowdermilk *et al.* [17], and classified the data to four flow regimes. According to Katto, a nonlinear

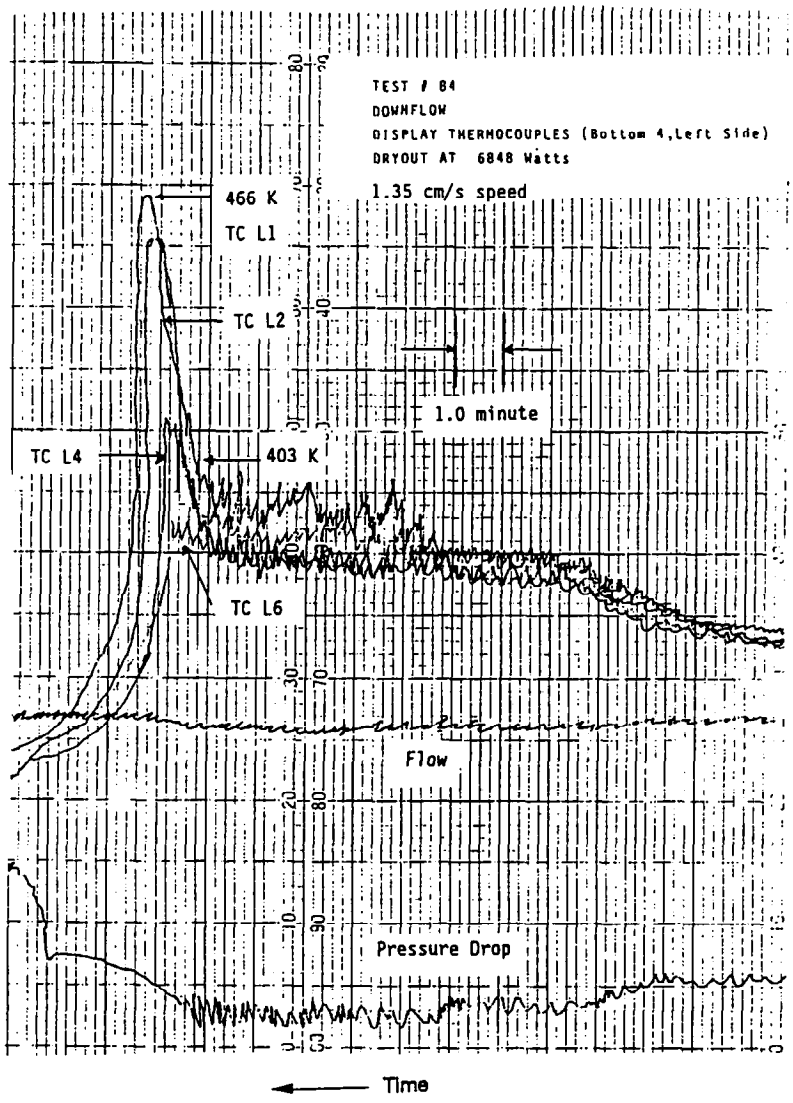

FIG. 4. Strip chart of substrate temperatures. (TC L1 to TC L6 denote the distance of left thermocouples from $z = 0$ measured in inches.)

regime occurs where the flow rate is very high, classified as the N-regime. This regime appears to belong to Type B in Fig. 5(a). Type A in Fig. 5(a) was found in the L-regime where the flow rate is low and is represented by a dimensionless $\sigma\rho_f/G^2L$ between 10^{-5} and 10^{-1}. Our data would fit Type A because our flow rates were within the specified range. Type C is represented by the VL-regime where the mass flow is lower than for the L-regime.

Figure 5(b) shows the effect of subcooling for upward flow as the mass flow rate increased for uniform heat flux distributions wherein the hot spot was located at the flow exit. As demonstrated in Fig. 5(b), the effect of subcooling was not significant in the thin rectangular channel, while mass flux influenced CHF significantly. The same trend was found by El-Genk *et al.* [13] for the small annuli tested (annulus ratios of 1.575 and 1.72).

Pressure

Typical CHF behavior is shown in Fig. 6(a) as a function of reduced pressure. Generally, CHF increases in region 'ab' up to a reduced pressure of 0.75 as the pressure increases, is relatively constant in region 'bc', and decreases in region 'cd' as the pressure increases. Although the optimum CHF occurs at reduced pressures in the vicinity of 0.75 as shown in Fig. 6(a), this location appears to vary somewhat with the mass flux as indicated by the dot–dash line based on the data correlation of Bowring [7]. Since our mass flow range was so low, thus simulating natural boiling, CHF increased as the pressure increased at constant inlet subcooling. The result is shown in Fig. 6(b).

Mass flux

Critical heat flux increases with mass flux. The relation is nearly linear between CHF and mass flux

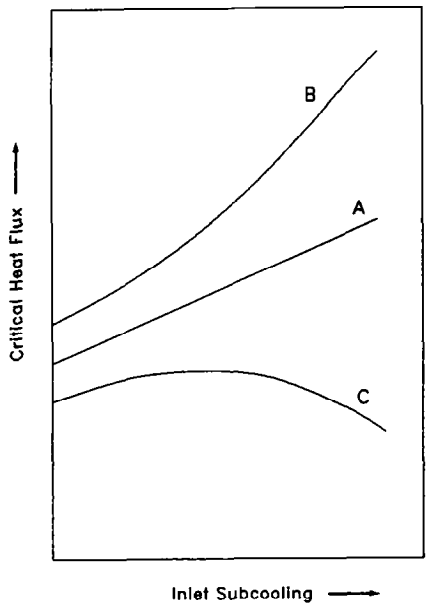

FIG. 5(a). Relationship between CHF and inlet subcooling [14].

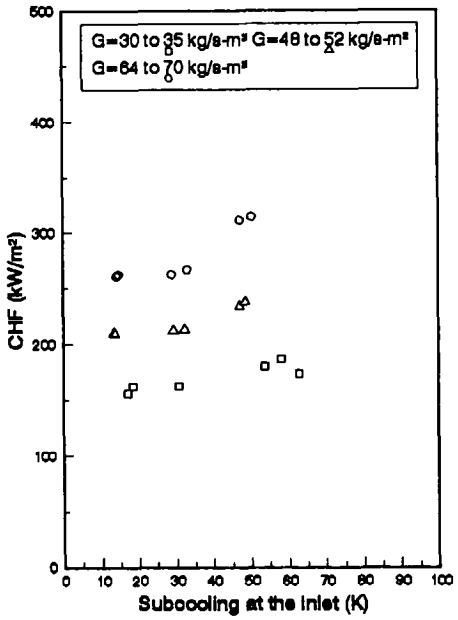

FIG. 5(b). Subcooling vs CHF as a variable of mass flux at 50 kPa for upward flow.

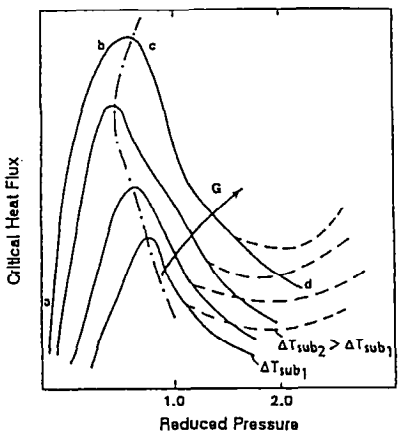

FIG. 6(a). Behavior of CHF and optimum CHF with respect to reduced pressure, with mass flux and subcooling as variables [7].

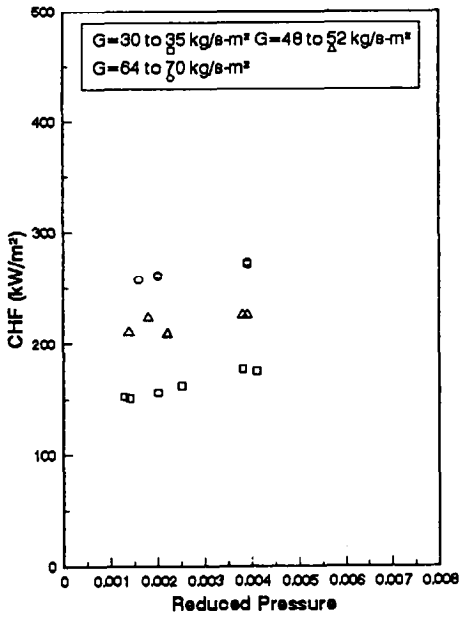

FIG. 6(b). Reduced pressure vs CHF as a variable of mass flux at an inlet water temperature of 338 K for upward flow.

in the low mass flux region, specifically less than 100 kg s^{-1} m^{-2}. Figure 7(a) exhibits CHF vs mass flux studied by Gambill [22] and Merilo [23] for their own data. The same trend was found in our study for the mass flux range of interest. Figure 7(b) shows CHF dependence on mass flux at three different sets of pressure and inlet temperature for the upward flow orientation. As shown, the effect of the inlet subcooling was not noticeable between $\Delta T_{sub} = 44$ and 27 K. However, as the inlet subcooling increases up to 66 K, the difference appears to be 15%. Figure 7(c) shows that CHF occurs at a 15% lower heat flux level in the downward flow than the upward flow. The same trend due to the flow direction was found by Kaminaga *et al.* [15].

COMPARISON OF TEST DATA WITH OTHER CORRELATIONS

Downward flow

Experimental CHF data in the present study were compared to CHF values calculated using the CHF

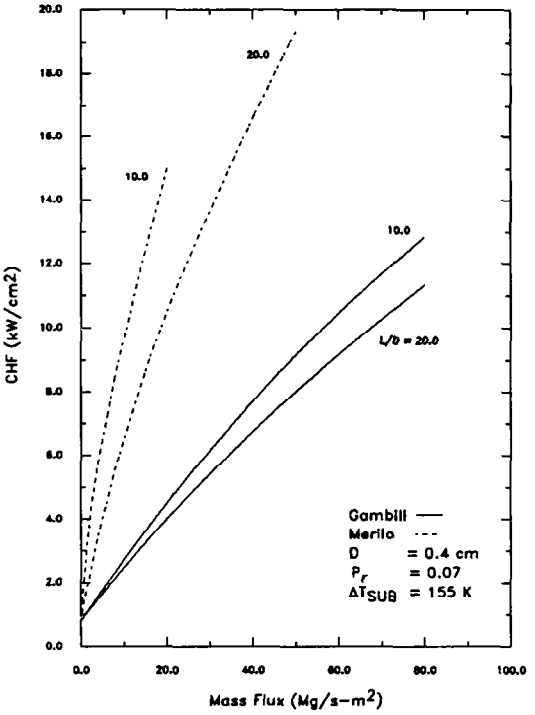

FIG. 7(a). Comparison of CHF predictions for subcooled flow, with respect to mass flux and with L/D as a parameter [22, 23].

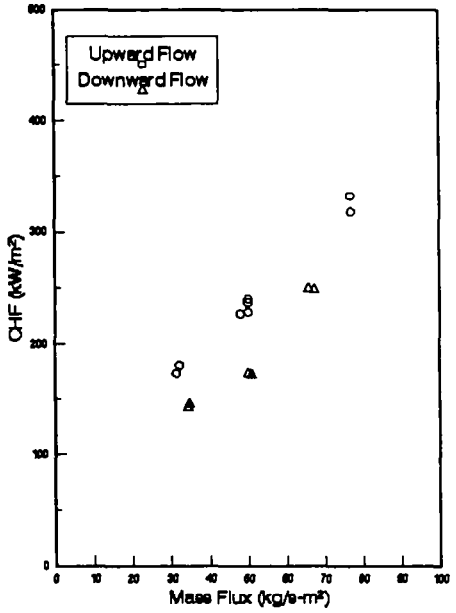

FIG. 7(c). CHF comparison between upward flow and downward flow at atmospheric pressure and 323 K water inlet temperature.

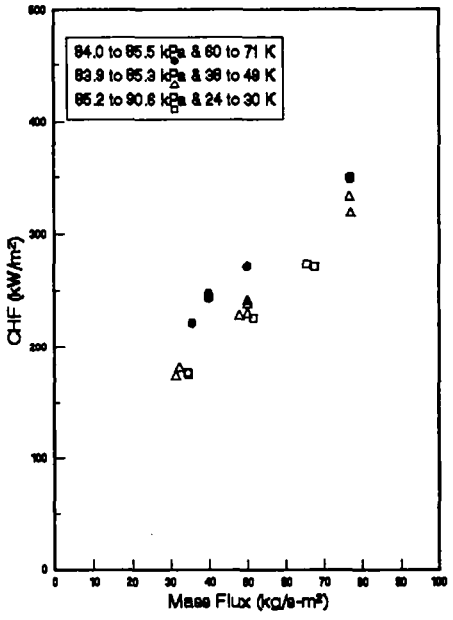

FIG. 7(b). Mass flux vs CHF at atmospheric pressure and various inlet subcooling for upward flow.

correlations referenced earlier. Again, those correlations developed for the low mass flow rate were used in these comparison calculations.

Figure 8(a) shows the comparison for exit pressure of 85 kPa and inlet water temperature of about 298 K (Δh_i = 278–302 kJ kg^{-1}). As shown in Fig. 8(a), the closest prediction of experimental CHF data was with the Lowdermilk correlation [17] with −30%, which was underpredicted by ~30%. The other CHF correlations also underpredicted our experimental CHF data by more than 30%.

One possible reason could be the different surface materials, i.e. Inconel 600 for Kaminaga *et al.* [15] and 304 stainless steel for the other investigators listed in Fig. 8(a). Other possible reasons could be the different flow geometry, operating conditions, length/diameter (L/D) ratio, inlet/outlet conditions, and unknown parameters such as oxide film build up. For example, the Katto correlation [14] was developed for a pressure range up to 6900 kPa, which is much higher than pressures used in this present study. The Mishima and Nishihara [10] correlation turned out to be the worst predictor in this comparison. Mishima and Nishihara's experimental CHF data apparently showed the relationship between mass flux and CHF. However, mass flux was not included for the downward CHF correlation. Therefore, as shown in Fig. 8(a), the Mishima and Nishihara correlation is insensitive to the mass flux. Also, for the mass flux range up to 100 kg s^{-1} m^{-2}, Mishima and Nishihara's data for downward flow showed smaller CHF values than those for upward flow by a factor of two. The reason for the significant discrepancy is unknown.

Upward flow

The hot spot occurred at a location where flow exits. Because the upward flow deals with the co-

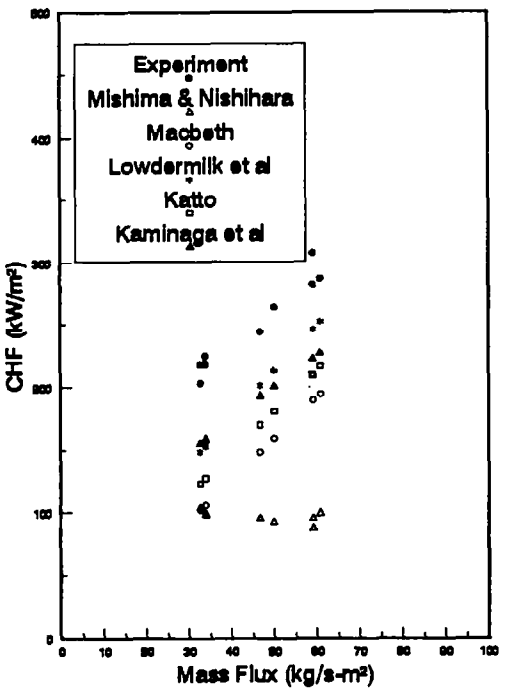

FIG. 8(a). Comparison of experimental CHF with other CHF correlations at atmospheric pressure and 298 K for downward flow.

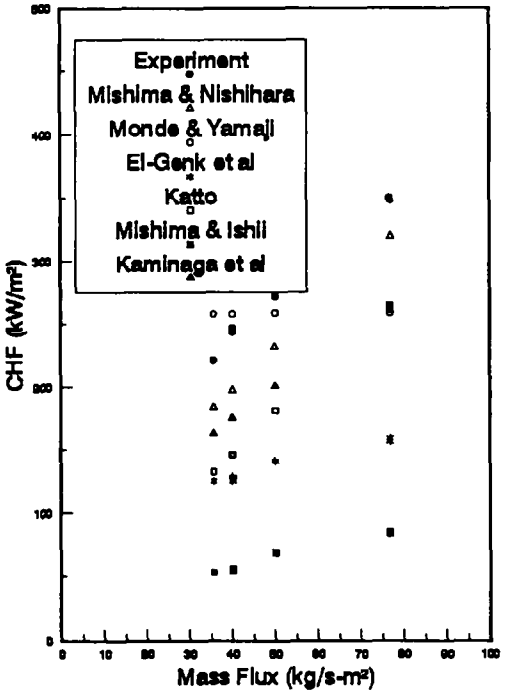

FIG. 8(b). Comparison of experimental CHF with other CHF correlations at atmospheric pressure and 298 K for upward flow.

current flow of steam–water, the transition of the flow regime was observed to be smoother than with the counter-current flow of steam–water associated with downward flow.

Figure 8(b) shows the comparison at system pressures from 84 to 86 kPa and an inlet water temperature of 298 K (Δh_i = 252–296 kJ kg^{-1}). Although pool boiling CHF was not included in the data plot, the pool boiling CHFs defined by Zuber [24] and Kutateladze [4] were higher than our experimental CHF by a factor of 2.5–3.5. This same trend is drawn by Monde and Yamaji [11]. As shown in Fig. 8(b), most CHF correlations underpredicted our experimental CHF by factors of two to four. Mishima and Nishihara's [10] prediction is the closest to experimental CHF data with an error bound of −8 to −19%. Monde and Yamaji [11] predict experimental CHF closely for a mass flux of 40–50 kg s^{-1} m^{-2}. However, at higher flow rates, CHF were underpredicted by Monde and Yamaji. This is the same trend indicated by Mishima and Ishii [12]. (When mass flux was lower than 40 kg s^{-1} m^{-2}, there appeared to be no difference between forced convection boiling and natural convection boiling. However, when mass flux increased, Mishima and Ishii's data indicated that forced convection had higher CHF values than those for natural convection.) Mishima and Ishii, and El-Genk *et al.* [13] carried out similar experiments to this present study. However, the predicted CHF values are much lower than those measured in the present study. The differences with the present study were the annular flow geometry (D_e = 0.0127 m for El-Genk *et al.* and D_e = 0.0055 m for Mishima and Ishii) vs thin rectangular channel (D_e = 0.00396 m for the present study), and 304 stainless steel surface material vs aluminum. The CHF data, based on the wide annuli, may not be applicable for those measured in the thin rectangular channel. The differences are at least understood.

DEVELOPMENT OF CRITICAL HEAT FLUX CORRELATIONS

Downward flow

Since downward flow CHF depends on the two-phase counter-current flow limit (CCFL), particular attention was paid to CCFL phenomena, specifically at the top of the test section where the subcooled water entered and saturated steam exited. Although no significantly reduced inlet flow of water was observed since water was fed to the test section by forced flow, CHF conditions observed in the experiment were similar to a CCFL burnout. An energy balance in the heated test section at CHF was used to develop the following dimensionless expression for CHF [12]:

$$\left(\frac{A_h}{A}\right)q^* = \left[\left(\frac{1}{C_0} - 0.11\right)\sqrt{D^*} + \frac{\Delta h_i}{h_{fg}}G^*\right] \quad (1)$$

where

$$q^* = \frac{Q}{h_{fg} A_h \sqrt{(\lambda \rho_g g \Delta\rho)}}$$

$$D^* = D/\lambda$$

$$\lambda = \sqrt{\left(\frac{\sigma}{g\Delta\rho}\right)}$$

$$C_0 = 1.2 - 0.2\sqrt{\left(\frac{\rho_g}{\rho_f}\right)}. \quad (2)$$

The void distribution parameter C_0 [12] at the location of CHF would be different, unlike the flow in vertical tubes. (The CCFL model developed by Mishima and Nishihara [25] assumed that the liquid downflow was in a film along the narrower, unheated side walls of the channel, while the gas flow occupied the wide span of the rectangular channel.) Also, the value of C_0 whose correlation was developed for an air–water system would be different for a steam–water system. Because of the uncertainty associated with determining the correct value for C_0 for flow in a vertical thin rectangular channel, equation (1) was rewritten in the following empirical form:

$$\left(\frac{A_h}{A}\right) q^* = A_1 \left[B_1 + C_1 \frac{\Delta h_i}{h_{fg}} G^*\right]. \quad (3)$$

Equation (3) can be rewritten as

$$\left(\frac{A_h}{A}\right) q^* = D_1 \left[1 + \frac{\Delta h_i}{h_{fg}}\right] G^* + E_1 \quad (4)$$

where the coefficients D_1 and E_1 were determined from the least square fit of equation (4) to the experimental CHF data covering all parameter ranges examined in the present study for the downward flow: $D_1 = 0.406$ and $E_1 = 2.412$

$$\left(\frac{A_h}{A}\right) q^* = 0.406 \left(1 + \frac{\Delta h_i}{h_{fg}}\right) G^* + 2.412. \quad (5)$$

As Fig. 9(a) demonstrates, equation (5) is in good agreement with the CHF data; the deviation between the data and the correlation is within $\pm 19\%$.

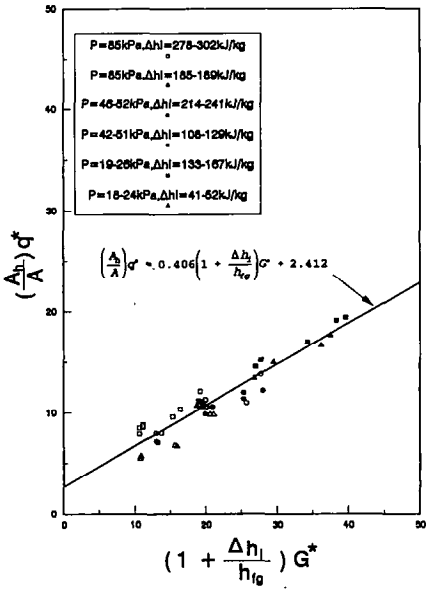

FIG. 9(a). CHF correlation for the downward flow.

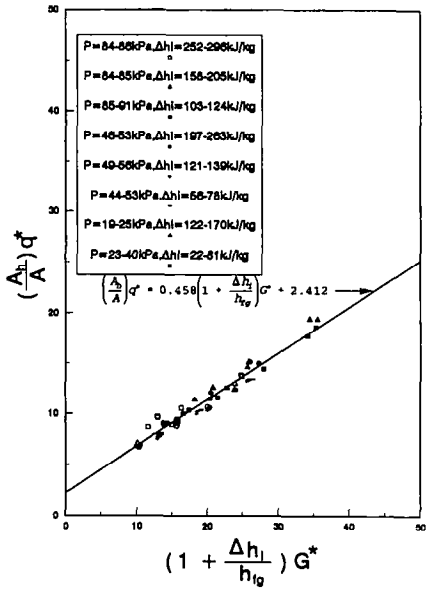

FIG. 9(b). CHF correlation for the upward flow.

Upward flow

The upward flow tests have co-current steam–water flow. The flow pattern transition from a churn to annular flow regime appears to be quicker than the downward flow. Unlike Mishima and Ishii, CHF did not occur at the transition of flow regime. At low flow, dryout occurred when the vapor quality at the exit reaches 100% in a heated channel. From the least square fit of equation (4) to CHF data for upward flow, the coefficients obtained were: $D_1 = 0.458$ and $E_1 = 2.412$

$$\left(\frac{A_h}{A}\right) q^* = 0.458 \left(1 + \frac{\Delta h_i}{h_{fg}}\right) G^* + 2.412. \quad (6)$$

Figure 9(b) shows that equation (6) is in good agreement with the data within $\pm 17\%$.

COMPARISON WITH HIGH FLOW CHF CORRELATIONS

Figure 10 compares equation (6) with the CHF correlations of Knoebel *et al.* [3], Groeneveld *et al.* [8] in RELAP5/MOD3 [26], and Biasi *et al.* [9]. As shown in Fig. 10, Biasi underpredicted the CHF data and is lower than other correlations. Shumway [27] compared Biasi and Groeneveld at low flow conditions (50 kg s^{-1} m^{-2}) over a range of pressures from 1 to 20 MPa with $\Delta T_{sub} = 10$ K. The Biasi predictions were much lower than Groeneveld's predictions by factors ranging from two to six. Most high flow CHF correlations like Groeneveld and Knoebel overpredicted CHF data. The probable difference may be attributed to high flow CHF correlations which,

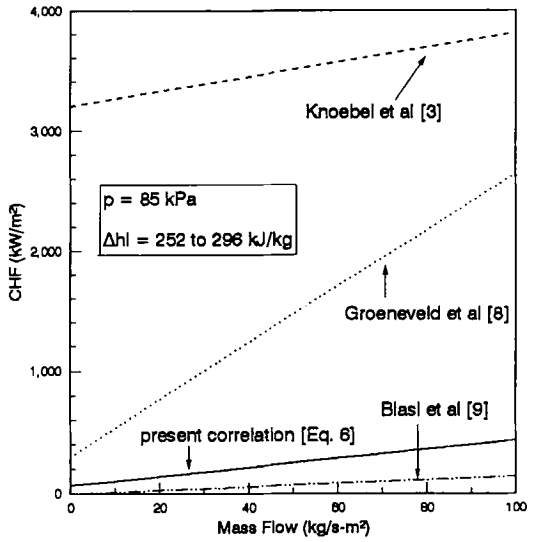

FIG. 10. Comparison of the present correlation with those of Knoebel *et al.* [3], Groeneveld *et al.* [8], and Biasi *et al.* [9].

though derived from a wide range of higher pressure and mass fluxes, are based on a limited low flow and low pressure data base. As shown in Fig. 10, the correlations of Knoebel *et al.* and Groeneveld *et al.*, when extrapolated to low flows and low pressures, significantly overestimate CHF data. Similarly, equations (5) and (6) should be applied up to 100 kg s^{-1} m^{-2}.

CONCLUSIONS

Steady-state CHF experiments were carried out for low flow and low pressure conditions simulating natural convection conditions in a vertical, thin, rectangular, aluminum, flow channel (L/D ratio of 154). Both upward and downward flow CHF data were collected for ranges of exit pressures (20–85 kPa), mass fluxes (30–80 kg s^{-1} m^{-2}), and inlet subcooling (22–302 kJ kg^{-1}). The test channel had a gap width of 0.00198 m, a heated width of 0.0508 m and a heated length of 0.6096 m.

Based on results of this present study, the following conclusions were drawn:

(1) The experimental CHFs did not agree well with existing correlations developed for low flow and low pressure conditions. These correlations are limited to atmospheric pressure, and no data are available for subatmospheric pressure, which may be an important parameter in natural convection CHF.

(2) New CHF correlations were developed for upward flow (equation (5)) and downward flow (equation (6)). These correlations agree with our experimental results with a maximum error band of 19% for downward flow and 17% for upward flow.

(3) Most high flow dryout CHF correlations, such as Groeneveld and Knoebel, overestimated low flow CHF data when extrapolated to low flow rates.

(4) The downward flow produced a CHF at least 15% lower than the upward flow. The same trend was found by Kaminaga *et al.* [15].

(5) The effect of subcooling for less than 44 K was not significant in the thin rectangular channel. As subcooling increased up to 66 K, CHF increased by 15%.

Acknowledgements—Work was performed under the auspices of the U.S. Department of Energy, Assistant Secretary for Nuclear Energy, Office of Nuclear Energy, under the DOE Idaho Field Office, Contract No. DE-AC07-76IDO1570.

REFERENCES

1. M. L. Griebenow and G. H. Hanson, ATR core-1 thermal-hydraulics test results, Idaho National Engineering Laboratory, TR-727 (1976).
2. L. Bernath, A theory of local boiling burnout and its application to existing data, *Chem. Engng Prog. Symp. Ser.* **56**(30), 95–116 (1960).
3. D. H. Knoebel, S. D. Harris and B. Crain, Forced convection subcooled critical heat flux, D_2O and H_2O coolant with aluminum and stainless steel heaters, Savannah River Laboratory, P-1306 (1973).
4. S. S. Kutateladze, Elements of hydrodynamics of gas–liquid systems, *Fluid Mech.—Sov. Res.* **1**, 29–50 (1972).
5. A. E. Bergles and W. M. Rohsenow, The determination of forced-convection surface-boiling heat transfer, *J. Heat Transfer* **86**, 365–372 (1964).
6. W. H. Jens and P. A. Lottes, Analysis of heat transfer, burnout, pressure drop, and density data for high pressure water, U.S. AEC, ANL-4627 (1951).
7. W. R. Bowring, Round tube, uniform heat flux, dryout correlation for water, U.K. AEEW-R 5055 (1972).
8. D. C. Groeneveld, S. C. Cheng and T. Doan, 1986 AECL-UO critical heat flux lookup table, *Heat Transfer Engng* **7**(1–2), 46–62 (1986).
9. L. Biasi, G. C. Clerici, S. Garribba, R. Sala and A. Tozi, Studies on burnout part 3—a new correlation for round ducts and uniform heating and its comparison with world data, *Energia Nucleare* **XIV**(9), 530–536 (1967).
10. K. Mishima and N. Nishihara, The effect of flow direction and magnitude on CHF for low pressure water in thin rectangular channels, *Nucl. Engng Des.* **86**, 165–181 (1985).
11. M. Monde and K. Yamaji, Critical heat flux during natural convective boiling in vertical uniformly heated tubes submerged in saturated liquid, 9th Int. Heat Transfer Conf., 1-BO-19, pp. 111–116 (1991).
12. K. Mishima and M. Ishii, Critical heat flux experiments under low flow conditions in a vertical annulus, NUREG/CR-2647, ANL-82-6 (1982).
13. M. S. El-Genk, S. J. Haynes and S. Kim, Experimental studies of critical heat flux for low flow of water in vertical annuli at near atmospheric pressure, *Int. J. Heat Mass Transfer* **31**, 2291–2304 (1988).
14. Y. Katto, A generalized correlation of critical heat flux for the forced convection boiling in vertical uniformly heated round tubes, *Int. J. Heat Mass Transfer* **21**, 1527–1542 (1978).
15. M. Kaminaga, Y. Sudo and Y. Muratama, Experimental study of the critical heat flux in a narrow vertical rectangular channel, *Heat Transfer Jap. Res.* **20**(1), 72–85 (1991).
16. R. V. Macbeth, Burnout analysis part 4: application of a local conditions hypothesis to world data for uniformly

heated round tubes and rectangular channels, AEEW-R267 (1963).
17. W. H. Lowdermilk, C. D. Lanzo and B. L. Siegel, Investigation of boiling burnout and flow instability for water flowing in tubes, NACA-TN-4382 (1958).
18. P. D. Bayless, ATR large-break LOCA best-estimate analysis, *Trans. ANS* **59**, 190 (1989).
19. F. Tachibana, M. Akiyama and H. Kawamura, Non-hydrodynamic aspects of pool boiling burnout, *J. Nucl. Sci. Technol.* **4**, 121–130 (1967).
20. H. J. Van Ouwerkerk, Burnout in pool boiling, the stability of boiling mechanism, *Int. J. Heat Mass Transfer* **15**, 25–33 (1972).
21. J. A. Block and G. B. Wallis, Heat transfer and fluid flows limited by flooding, *A.I.Ch.E. Symp. Ser. No. 174* **74**, 73–82 (1978).
22. W. R. Gambill, Burnout in boiling heat transfer part II: subcooled forced-convection system, *Nucl. Safety* **9**(6), 467–480 (1968).
23. M. Merilo, Critical heat flux experiments in a vertical and horizontal tube with both Freon-12 and water as coolant, *Nucl. Engng Des.* **44**, 1–16 (1977).
24. N. Zuber, Hydrodynamic aspects of boiling heat transfer, AECU-4439 (1959).
25. K. Mishima and H. Nishihara, Flooding velocity for countercurrent air–water in rectangular channels, *A. Rep. Res. Reactor Inst. Kyoto Univ.* **17**, 1–4 (1984).
26. K. E. Carlson, R. A. Riemke, S. Z. Rouhani, R. W. Shumway and W. L. Weaver, RELAP5/MOD3 Code Manual, EG&G Idaho, Inc., NUREG/CR-5535, EGG-2596 (1990).
27. R. Shumway, New critical heat flux method for RELAP5/MOD3, EG&G Idaho, Inc., EGG-EAST-8443 (1989).